INTERNATIONAL JOURNAL FOR NUMERICAL AND ANALYTICAL METHODS IN GEOMECHANICS, VOL. 22, 49–71 (1998)

AN EXAMINATION OF THE VALIDATION OF A MODEL OF THE HYDRO/THERMO/MECHANICAL BEHAVIOUR OF ENGINEERED CLAY BARRIERS

H. R. THOMAS[1]*, Y. HE[1] AND C. ONOFREI[2]

[1] *Cardiff School of Engineering, University of Wales Cardiff, P.O. Box 925, Cardiff, CF2 1YF, U.K.*
[2] *Whiteshell Laboratories, Pinawa, Manitoba R0E 1L0, Canada*

SUMMARY

This paper focuses attention on the development of a numerical model of the hydro/thermo/mechanical behaviour of unsaturated clay and its consequent verification and validation. The work presented describes on-going collaboration between the Cardiff School of Engineering and Atomic Energy of Canada. The model development, which was carried out at Cardiff, can be described as being based on a mechanistic approach to coupled heat, moisture and air flow. This is then linked to a deformation analysis of the material within a 'consolidation' type of model. The whole is solved via the finite element method to yield a computer software code named COMPASS (COde for Modelling PArtly Saturated Soil). Some aspects of verification and validation of the model have been addressed in-house. However, the purpose of current AECL work is to provide an independent, rigorous, structured programme of validation and the paper will also explore the further validation of COMPASS within this context. © 1998 by John Wiley & Sons, Ltd.

Int. J. Numer. Anal. Meth. Geomech., Vol. 22, 49–71 (1998)
(No. of Figures: 11 No. of Tables: 0 No. of Refs: 25)

Key words: unsaturated soil; heat transfer; moisture transfer and stress–strain behaviour; model and validation

1. INTRODUCTION

A comprehensive analysis of coupled heat and moisture transfer in a deformable unsaturated soil remains a major research problem of interest in nuclear waste disposal. In particular, in order to obtain an improved understanding of the behaviour of the engineered clay barrier, heat transfer, moisture migration, air transfer, stress equilibrium and stress–strain behaviour need to be considered. Since the interrelated effects of these various phenomena are too complicated for an analytical solution to be achieved, an effective numerical approach has to be employed for the modelling work.

Coupled heat and moisture transfer in a rigid porous media under gradients of temperature and moisture content has been extensively studied based on a model originally proposed by Philip and de Vries.[1] Adopting a mechanistic approach based on the microscopic phase interaction of the liquid, vapour and porous structure, de Vries[2] developed the theory further and

*Correspondence to H. R. Thomas, Cardiff Echool of Engineering, University of Wales Cardiff, P.O. Box 925, Cardiff, CF2 1YF, U.K.

CCC 0363–9061/98/010049–23$17.50

Received 30 March 1997
Revised 4 April 1997

presented a detailed formulation for coupled heat and moisture transfer in a rigid porous medium under the influence of gradients of temperature and moisture. The approach has established itself in the literature and a significant number of papers on heat and mass transfer in porous media have subsequently appeared based on solutions of the model and its further development and extension.[3–7]

The stress–strain behaviour of unsaturated soil has been the subject of numerous experimental and theoretical investigations. A number of constitutive relationships have been proposed to describe soil behaviour,[8–10] incorporating the so-called state surface approach and more recently elasto-plastic type models.

The concept of a state surface was first suggested by Bishop and Blight.[11] Fredlund[12] proposed constitutive equations to describe a state surface using the logarithmic form. Further development of the state surface approach were reported by Lloret and Alonso.[13]

The advantage of the state surface approach is that both wetting collapse and swelling characteristics due to the effect of suction and stress interaction can be accommodated. The uniqueness of the state surface for the void ratio and degree of saturation has been experimentally verified by Matyas and Radhakrishna[14] for the case of monotonic changes in net stress and suction. However, experimental observations indicate that this unique relationship is lost if soil is subjected to loading/unloading or wetting/drying cycles, which give rise to hysteresis effect.

An elasto-plastic model was proposed by Alonso *et al.*[9] formulated within the framework of strain hardening plasticity using net mean stress and suction as its primary stress variables. The model is able to represent many features of unsaturated soil in a consistent and unified manner. Combined with a soil liquid flow balance equation and a stress equilibrium equation, it can be applied to simulate the wetting-loading collapse and drying shrinkage behaviour of unsaturated soil. When saturation is reached, the model becomes a conventional critical state model.

Liquid, vapour, air and heat transfer occur simultaneously in soil. The approach presented here treats each flow independently and relates the velocities of flow to the gradients of relevant potentials using the generalized laws of Darcy and Fourier. Both a non-linear elastic state surface approach and an elasto-plastic constitutive model have been incorporated in the work performed.

Having developed a model of the hydro/thermo/mechanical behaviour of unsaturated soil, its accuracy, both in terms of software integrity and its ability to describe the relevant physical phenomena, is matter of interest. Within the context of the safe disposal of high-level nuclear waste, such issues are clearly of paramount importance. This paper therefore also addresses same aspects of verification and validation of the model, both within conventional academic consideration and also the Canadian Nuclear Fuel Waste Management Program.

2. VALIDATION OF NUMERICAL MODELS FOR USE IN THE EVALUATION OF AN ENGINEERED CLAY BARRIER SYSTEM—GENERAL CONCEPTS

The Canadian Nuclear Fuel Waste Management Program (CNFWMP) is evaluating the concept of disposal of nuclear fuel waste in an engineered vault at a depth of 500 to 1000 m in the plutonic rock of the Canadian Shield. In the engineered barrier system designs being developed, the waste would be contained within durable containers that, in turn, would be isolated from the host rock by clay-based materials.

Both the design and the performance assessment rely on experiments performed on physical models of vault elements over relatively short times and on information inferred from calculations (mathematical models) that simulate the probable behaviour of the system in the space–time domain of interest. Within CNFWMP, one of the more important goals is to determine whether the simulation models used are adequate tools that represent the probable behaviour of the real engineered barriers.

The general procedure used in the analysis of an engineering barrier system is based on system analysis, where the starting-point of the analysis is a conceptual system, which, by definition, is an abstraction. A simulation model that simplifies the conceptual system is developed, in which numerical values are given to the general statements of size, magnitude and influences. After the simulation model is judiciously tested (validated) it is used as a direction to build the new product, the concrete object. The end product is in a sense a model of the conceptual system, and the simulation model sits between the concept and physical reality. Obviously, a comparison of the simulation model outputs with measurements of the concrete object before the object is built is not possible. Difficulties encountered in the validation of a simulation model are generally resolved by developing physical models of the conceptual system or of components of the system, and testing the model by comparing the outputs from a simulation with the outputs of a physical model.

The focal goal of the validation activity is to establish in a transparent fashion the process by which the repository developers will demonstrate a level of confidence in models used to estimate the probable behaviour of engineered clay barriers. The validation term, with its pragmatic meaning, is used in the programme to define the activity of testing these models that will lead to a reasonable assurance that the simulation results are acceptable. In this context, validation is concerned with the aspects of appropriateness and plausibility of a model to be used in solving practical problems. Results from a series of tests performed within this activity will serve as tangible evidence regarding the success of the model in representing the system of interest. If a simulation model is to be successful, that is, used within a real-world situation, it must give information or predictions that are clearly better, in some way, than the mental image or other abstracted model that would be used instead. The validation phase is the interface between model development and model application. Results from a series of tests performed within this activity will serve as tangible evidence regarding the success or the degree of success of a model in representing the system of interest.

COMPASS and several other models are included in the validation programme. Several facets of model validity are considered in this programme. Two types of validity, the so called event validity and face validity, are the most convincing tests regarding the usefulness of simulation models. Event validity, i.e. 'validation through model testing with experiments' is essential since a model derived from theory, no matter how elegant in itself, is unlikely to be of use solving a practical problem unless there is a practical way of assessing how well the theory agrees with the observed data. An event in this interpretation is an occurrence related to a concrete object; to each event belongs its place co-ordinates and time values. The tests included in this state are based on comparisons of model outputs with the outputs (measurements) of physical models of engineered barriers. In order to secure the integrity of these tests, a completely independent data set, other than data sets used in calibration and sensitivity analysis, are employed. The experiments within this activity are essentially of the same type as those used in the model development phase: (a) bench laboratory models, (b) large-scale laboratory models, and (c) *in situ* models. COMPASS preliminary tests results (event validity) using *in situ*

test of the isothermal experiment installed at AECL Underground Research Laboratory (URL) are presented in this paper.

Face validity that is concerned with the impression of realism that the simulation makes on the participants in the validation and application stage is also important since a simulation model, and in general any mathematical model, is an adjunct, a supporter to professional judgement, and never a substitute. Tests performed at this stage are primarily based on the intuition of engineers. Therefore they are, to some extent, subjective. However, it is important to emphasize that the results of all tests performed within the validation phase are checked continuously against the engineers' intuition. In this manner, face validity consolidates all other facets of the validation phase. The validation phase is designed to start and to end with face validity. Agreement between mathematics (simulation results) physical confirmation and intuition is regarded as a strong indication that the simulation is successful. Alternatively, disagreement is regarded as a signal for a need for the improvement of the existing models.

3. HYDRO/THERMO/MECHANICAL BEHAVIOUR OF UNSATURATED CLAY—BASIC THEORY

3.1. Stress–strain constitutive relationship and governing equation

When employing a state surface approach, total strain is assumed to consist of components due to net stress, suction and temperature changes. This can be given in an incremental form, without loss of generality, as

$$d\varepsilon = d\varepsilon_\sigma + d\varepsilon_s + d\varepsilon_T \tag{1}$$

where the subscripts σ, s and T refer to the net stress, suction and temperature, respectively.

The net mean stress and suction are chosen as the primary variables of the state surface for void ratio. Lloret and Alonso[13] examined a number of forms of state surfaces of void ratio and concluded that the following formulation gives an accurate description of soil behaviour:

$$e = e_0 + a' \ln(p) + b' \ln(s_r) + c' \ln(p)\ln(s_r) \tag{2}$$

where e is void ratio, s_r is the suction at the reference temperature T_r, a', b' and c' are constants.

The stress state variables p and s can be defined as[10]

$$p = \tfrac{1}{3}(\sigma_x + \sigma_y + \sigma_z) - u_a \tag{3}$$

$$s = u_a - u_l \tag{4}$$

where u_l is the pore liquid pressure and u_a is the pore air pressure.

In the model developed here, temperature influence on the volumetric strain includes the contributions of (i) thermal expansion and (ii) suction change due to temperature effect via surface energy.

The elastic deviatoric strain induced by the deviatoric stress change q will be evluated through a shear modulus G.

$$d\varepsilon_q = dq/3G \tag{5}$$

Combining the above equations, the stress–strain relationship may be expressed as

$$d\underline{\sigma}'' = \mathbf{D}(d\underline{\varepsilon} - d\underline{\varepsilon}_s - d\underline{\varepsilon}_T) \tag{6}$$

where σ'' is the net stress which is defined as

$$\mathrm{d}\underline{\sigma}'' = \mathrm{d}(\underline{\sigma} - u_\mathrm{a}) \tag{7}$$

and $\mathbf{D}$ is the elastic matrix.

The governing stress equilibrium equation for non-isothermal deformation in an isotropic elastic unsaturated porous medium subjected to small deformation is given as follows:

$$\frac{\partial(\mathrm{d}\sigma_{ij})}{\partial x_j} + \mathrm{d}b_i = 0 \tag{8}$$

where b_i is the body force. Substituting equations (6) and (7) into equation (8) yields

$$\frac{\partial}{\partial x_j}(\mathbf{D}(\mathrm{d}\underline{\varepsilon} - \mathbf{A}_\mathrm{s}\,\mathrm{d}s - \mathbf{A}_\mathrm{T}\mathrm{d}T)) + \frac{\partial \mathrm{d}u_\mathrm{a}}{\partial x_j} + \mathrm{d}b_i = 0 \tag{9}$$

where $\mathbf{A}_\mathrm{s}$ is a suction matrix derived from the state surface of void ratio, $\mathbf{A}_\mathrm{T}$ is a thermal matrix that depends on the thermal expansion coefficient of soil and the surface energy of the soil–water system.

Experimental work indicates that significant irreversible deformation may be induceed when wetting/collapse takes place in unsaturated soil. Furthermore large increases in suction may also induce plastic strain. An elasto-plastic model is therefore required to accommodate these features.

In an elasto-plastic approach, total strain is assumed to include plastic components due to net stress, suction and temperature changes, that is

$$\mathrm{d}\varepsilon = \mathrm{d}\varepsilon_\sigma^\mathrm{e} + \mathrm{d}\varepsilon_\mathrm{s}^\mathrm{e} + \mathrm{d}\varepsilon_\mathrm{T}^\mathrm{e} + \mathrm{d}\varepsilon^\mathrm{p} \tag{10}$$

where the superscripts e and p refer to the elastic and plastic strains respectively. The stress–strain relationship can be expressed as

$$\mathrm{d}\underline{\sigma}'' = \mathbf{D}(\mathrm{d}\underline{\varepsilon} - \mathrm{d}\underline{\varepsilon}_\mathrm{s}^\mathrm{e} - \mathrm{d}\underline{\varepsilon}_\mathrm{T}^\mathrm{e} - \mathrm{d}\underline{\varepsilon}^\mathrm{p}) \tag{11}$$

Appropriate yield equations and plastic potentials need to be defined for the evaluation of the plastic strain. In the work presented here, the elasto-plastic constitutive relationship proposed by Alonso *et al.*[9] is employed to determine the volumetric plastic strain.

Substituting equation (11) into equation (8) yields

$$\frac{\partial}{\partial x_j}(\mathbf{D}(\mathrm{d}\underline{\varepsilon} - \mathbf{A}_\mathrm{s}\mathrm{d}s - \mathbf{A}_\mathrm{T}\,\mathrm{d}T - \mathrm{d}\underline{\varepsilon}^\mathrm{p})) + \frac{\partial \mathrm{d}u_\mathrm{a}}{\partial x_j} + \mathrm{d}b_i = 0 \tag{12}$$

Equation (12) is the governing equation for the elasto-plastic model. Unlike the previous elastic approach, the method requires an iterative procedure to obtain the correct irreversible deformation.

3.2. Moisture mass transfer

The volumetric moisture content in unsaturated soil is defined as the sum of the volumetric liquid content and the volumetric vapour content.

$$\theta = \theta_\mathrm{l} + \theta_\mathrm{v} \tag{13}$$

where θ_l and θ_v are the volumetric content of liquid and vapour respectively. Moisture transfer in unsaturated soil can therefore be considered in two parts, liquid transfer and vapour transfer. Considering the combined effects of the movement of liquid, the movement of vapour due to vapour diffusion together with the movement of vapour in the pore air, the law of conservation of mass for the moisture dictates that

$$\frac{\partial(\theta_l \rho_l)}{\partial t} + \frac{\partial(\theta_a \rho_v)}{\partial t} + \nabla \cdot (\underline{v}_l \rho_l) + \nabla \cdot (\underline{v}_v \rho_l) + \nabla \cdot (\underline{v}_a \rho_v) = 0 \tag{14}$$

where ρ is the density, t is the time and $\underline{v}$ is the velocity. The subscripts l, a and v refer to liquid, air and water vapour, respectively. θ_l and θ_a are defined by

$$\theta_l = nS_l \tag{15}$$

$$\theta_a = n - \theta_l \tag{16}$$

where n is the porosity and S_l is the degree of saturation with respect to the pore liquid.

In this model the soil is deformable, therefore the variation of porosity must be included. It is necessary therefore to rewrite equation (14) in terms of porosity and degree of saturation as follows

$$\frac{\partial(nS_l \rho_l)}{\partial t} + \frac{\partial(nS_a \rho_v)}{\partial t} + \nabla \cdot (\underline{v}_l \rho_l) + \nabla \cdot (\underline{v}_v \rho_l) + \nabla \cdot (\underline{v}_a \rho_v) = 0 \tag{17}$$

The motion of pore liquid can be defined according to a generalised Darcy's law.[14]

The degree of saturation of pore water may be assumed to be dependent exclusively on the suction and net mean stress in unsaturated soil.[8,10]

$$S_l = S_l(p, s, T)$$

The state surface approach is again employed to relate the degree of saturation of pore liquid to net mean stress, suction and temperature. Noting that suction is a function of temperature via surface energy and differentiating the degree of saturation with respect to time yields

$$\frac{\partial S_l}{\partial t} = \frac{\partial S_l}{\partial p}\frac{\partial p}{\partial t} + \frac{\partial S_l}{\partial s}\frac{\partial s}{\partial t} + \frac{\partial S_l}{\partial T}\frac{\partial T}{\partial t} \tag{18}$$

Considering vapour diffusion, flow is assumed to occur under a vapour density gradient. An extended vapour velocity equation proposed by Thomas and King[6] is employed, i.e.

$$\underline{v}_v = -\left\{\frac{nD_{atm} v_v}{\rho_l}\left[\frac{\partial \rho_v}{\partial \psi}\nabla\psi + \frac{(\nabla T)_a}{\nabla T}\frac{\partial \rho_v}{\partial T}\nabla T\right]\right\} \tag{19}$$

where $\underline{v}_v$ is the velocity of vapour flow, n is porosity, D_{atm} is the molecular diffusivity for vapour through air, v_v is the mass flow factor, ρ_v is the density of the water vapour and ψ, the capillary potential, is defined as

$$\psi = (u_l - u_a)/\gamma_l \tag{20}$$

The velocity of vapour can be written in a more convenient form as follows:

$$\underline{v}_v = -\{K_{vl}\nabla u_l + K_{vT}\nabla T + K_{va}\nabla u_a\} \tag{21}$$

where K_{vl}, K_{vT} and K_{va} are functions of the capillary potential and temperature.

By the application of the generalized Darcy's law for multiphase flow in unsaturated soil,[15] the velocity of pore air is assumed to be governed by

$$\underline{v}_{\mathrm{a}} = -K_{\mathrm{a}}\nabla(u_{\mathrm{a}}) \tag{22}$$

Substituting (18), (21) and (22) into equation (17), the equation of moisture transfer can be finally written in the form of primary variables

$$C_{\mathrm{ll}}\frac{\partial u_{\mathrm{l}}}{\partial t} + C_{\mathrm{lT}}\frac{\partial T}{\partial t} + C_{\mathrm{la}}\frac{\partial u_{\mathrm{a}}}{\partial t} + C_{\mathrm{lu}}\frac{\partial \underline{u}}{\partial t} = \nabla\left[K_{\mathrm{ll}}\nabla u_{\mathrm{l}}\right] + \nabla(K_{\mathrm{lT}}\nabla T) + \nabla\left[K_{\mathrm{la}}\nabla u_{\mathrm{a}}\right] + J_{\mathrm{l}} \tag{23}$$

where $\underline{u}$ is the vector of nodal displacements and C_{lj}, $K_{\mathrm{l}j}$ and J_{l} are coefficients of the equation ($j = \mathrm{l}, T, \mathrm{a}, \mathrm{u}$; with u in this case representing displacements in general).

3.3. Dry air mass transfer

Using Henry's law to take account of dissolved air in the pore water, conservation of dry air flow dictates that

$$\frac{\partial\left[\rho_{\mathrm{da}}(\theta_{\mathrm{a}} + H_{\mathrm{c}}\theta_{\mathrm{l}})\right]}{\partial t} + \nabla\cdot\left[\rho_{\mathrm{da}}(\underline{v}_{\mathrm{a}} + H_{\mathrm{c}}\underline{v}_{\mathrm{l}})\right] = 0 \tag{24}$$

where H_{c} is Henry's coefficient of solubility, ρ_{da}, the density of the dry air, is assumed to be given by

$$\rho_{\mathrm{da}} = \frac{u_{\mathrm{a}}}{R_{\mathrm{da}}T} - \frac{R_{\mathrm{v}}}{R_{\mathrm{da}}}\rho_{\mathrm{v}} \tag{25}$$

where R_{da} is the specific gas constant for dry air.

As stated previously, the velocity of pore air in the continuous air phase form is assumed to be described by equation (22)[16].

Substituting equations (15) and (16) into equation (24) yields

$$n\rho_{\mathrm{da}}\frac{\partial S_{\mathrm{a}}}{\partial t} + H_{\mathrm{c}}n\rho_{\mathrm{da}}\frac{\partial S_{\mathrm{l}}}{\partial t} + n\left(S_{\mathrm{a}} + H_{\mathrm{c}}S_{\mathrm{l}}\right)\frac{\partial \rho_{\mathrm{da}}}{\partial t} + \rho_{\mathrm{da}}\left(S_{\mathrm{a}} + H_{\mathrm{c}}S_{\mathrm{l}}\right)\frac{\partial n}{\partial t} = \nabla\cdot\left[\rho_{\mathrm{da}}(\underline{v}_{\mathrm{a}} + H_{\mathrm{c}}\underline{v}_{\mathrm{l}})\right] \tag{26}$$

The governing equation of dry air transfer in primary variable form therefore becomes

$$C_{\mathrm{al}}\frac{\partial u_{\mathrm{l}}}{\partial t} + C_{\mathrm{aT}}\frac{\partial T}{\partial t} + C_{\mathrm{aa}}\frac{\partial u_{\mathrm{a}}}{\partial t} + C_{\mathrm{au}}\frac{\partial \underline{u}}{\partial t} = \nabla\left[K_{\mathrm{al}}\nabla u_{\mathrm{l}}\right] + \nabla\left[K_{\mathrm{aa}}\nabla u_{\mathrm{a}}\right] + J_{\mathrm{a}} \tag{27}$$

where $C_{\mathrm{a}j}$, $K_{\mathrm{a}j}$ and J_{a} are coefficients of the equation ($j = \mathrm{l}, \mathrm{T}, \mathrm{a}, \mathrm{u}$).

3.4. Heat transfer

From considerations of conservation of energy, the governing differential equation for heat transfer can be written as

$$\frac{\partial \Phi}{\partial t} + \nabla\cdot\mathbf{Q} = 0 \tag{28}$$

where **Q** is the global heat flux per unit volume and Φ, the heat capacity of the soil per unit volume is defined as

$$\Phi = n(\rho_l S_l C_{pl} + \rho_v S_a C_{pv} + \rho_a S_a C_{pa})(T - T_r) + (1 - n)\rho_s C_{ps}(T - T_r) + n\rho_v S_a L \quad (29)$$

C_{pl}, C_{pv}, C_{pa} and C_{ps} are the specific heat capacities of pore liquid, pore water vapour, pore air and the solid particles respectively, T and T_r are the temperature and reference temperature respectively, ρ_s is the density of the solid particles and L is the latent heat of vaporization.

The heat flux per unit volume, including conduction, convenction and transfer of latent heat in vapour form, is defined according to

$$\mathbf{Q} = -\lambda_T \nabla T + (\rho_l \underline{v}_v + \rho_v \underline{v}_a)L + (C_{pl}\rho_l \underline{v}_l + C_{pv}\rho_l \underline{v}_v + C_{pv}\rho_v \underline{v}_a + C_{pa}\rho_a \underline{v}_a)(T - T_r) \quad (30)$$

where λ_T is the intrinsic thermal conductivity of the soil. Expanding equation (28) yields

$$H\frac{\partial T}{\partial t} + \frac{\partial H}{\partial t}(T - T_r) + LS_a\rho_v \frac{\partial n}{\partial t} + Ln\rho_v \frac{\partial S_a}{\partial t} + LnS_a \frac{\partial \rho_v}{\partial t} - \nabla\cdot(\lambda_T \nabla T) + L\rho_l \nabla(\underline{v}_v) + L\nabla\cdot(\underline{v}_a \rho_v)$$

$$+ \nabla\cdot[(C_{pl}\underline{v}_l\rho_l + C_{pv}\underline{v}_v\rho_l + C_{pv}\underline{v}_a\rho_v + C_{pda}\underline{v}_a\rho_{da})(T - T_r)] \quad (31)$$

where H, the specific heat capacity of the unsaturated soil, is defined as

$$H = (1 - n)C_{ps}\rho_s + n(C_{pl}S_l\rho_l + C_{pv}S_a\rho_v + C_{pda}S_a\rho_{da}) \quad (32)$$

Equation (31) can be finally written in primary variable form as

$$C_{Tl}\frac{\partial u_l}{\partial t} + C_{TT}\frac{\partial T}{\partial t} + C_{Ta}\frac{\partial u_a}{\partial t} + C_{Tu}\frac{\partial \underline{u}}{\partial t} = \nabla(K_{Tl}\nabla \underline{u}_l) + \nabla(K_{TT}\nabla T) + (\nabla K_{Ta}\nabla u_a)$$

$$+ V_{TT1}\cdot\nabla(T) + (T - T_r)\nabla\cdot(K_{Tl2}\nabla(u_l) + K_{TT2}\nabla(T) + K_{Ta2}\nabla(u_a)) + J_T \quad (33)$$

where C_{Tj}, K_{Tj}, V_{TT1} and J_T are coefficients of the equation, (j = l, T, a, u).

It is necessary to set up the initial and boundary conditions to solve the set of coupled equations. Boundary conditions take various forms as follows.

1. Prescribed primary variable $\phi = \phi^*$ on boundary S_d, where ϕ represents whole unknown. This is a Dirichlet condition.
2. Prescribed flux $q = q^*$ on boundary S_n. This is a Neumann condition.
3. Prescribed convection condition on boundary S_c, for example, $q = h(T - T_0)$ for temperature boundary. This is a Cauchy condition.
4. For the stress equilibrium equation, there can be loads from surface traction applied to boundary S_f.

With appropriate initial and boundary conditions, a set of coupled, non-linear governing equations is defined for the problem of heat and moisture transfer and deformation in unsaturated soil in terms of pore water pressure, pore air pressure, temperature and displacements.

4. HYDRO/THERMO/MECHANICAL BEHAVIOUR OF UNSATURATED CLAY—NUMERICAL MODELLING

There are several methods of formulating the finite element discretization of a set of governing differential equations, e.g. the variational method and the weighted residual method. The Galerkin weighted residual method is employed here. Quadratic quadrilateral elements are coded for pore water pressure, pore air pressure, temperature and displacement.

In the case of the mass or the energy balance equations, it is assumed that the approximation polynomial is given in terms of a shape function N_{m}. For simplicity, the transport equation is expressed in a brief form,

$$\frac{\partial(M_j)}{\partial t} + \nabla\cdot(\underline{q}_j) = 0 \tag{34}$$

where M refers to mass or enthalpy, $\underline{q}$ refers to the flux term, $j = \mathrm{l}, \mathrm{T}, \mathrm{a}$.

Through the Galerkin method, equation (34) can be discretized as follows:

$$\int_{\Omega}\left[N_{\mathrm{m}}^{\mathrm{t}}\frac{\partial(M_j)}{\partial t} - \nabla N_{\mathrm{m}}^{\mathrm{t}}\cdot(\underline{q}_j)\right]\mathrm{d}\Omega + \int_{\Gamma_2} N_{\mathrm{m}}^{\mathrm{t}}\underline{q}_j^{*}\,\mathrm{d}\Gamma = 0 \tag{35}$$

where q^* is the flux prescribed at boundary Γ_2 (Von Neumann boundary condition).

The stress equilibrium equation (9) for the non-linear elastic approach is discretized via the use of shape function N_{f}

$$\int_{\Omega}[\mathbf{B}^{\mathrm{t}}\mathbf{D}(\mathbf{B}\,\mathrm{d}u + \mathbf{A}_{\mathrm{s}}\,\mathrm{d}u_{\mathrm{l}} - \mathbf{A}_{\mathrm{s}}\,\mathrm{d}u_{\mathrm{a}} - \mathbf{A}_{\mathrm{T}}\,\mathrm{d}T)]\,\mathrm{d}\Omega - \int_{\Omega} N_{\mathrm{f}}^{\mathrm{t}}[\nabla \mathrm{d}u_{\mathrm{a}} + \mathrm{d}b_i]\,\mathrm{d}\Omega - \int_{\Gamma_2} N_{\mathrm{f}}^{\mathrm{t}}\underline{\tau}\,\mathrm{d}\Gamma = 0 \tag{36}$$

where $\mathbf{B}$ is the strain matrix and τ is the surface traction.

Similarly, discretization of the equilibrium equation (12) for the elasto-plastic approach yields

$$\int_{\Omega}[\mathbf{B}^{\mathrm{t}}\mathbf{D}(\mathbf{B}\,\mathrm{d}u + \mathbf{A}_{\mathrm{s}}\,\mathrm{d}u_{\mathrm{l}} - \mathbf{A}_{\mathrm{s}}\,\mathrm{d}u_{\mathrm{a}} - \mathbf{A}_{\mathrm{T}}\,\mathrm{d}T)]\,\mathrm{d}\Omega - \int_{\Omega} N_{\mathrm{f}}^{\mathrm{t}}[\nabla \mathrm{d}u_{\mathrm{a}} + \mathrm{d}b_i]\,\mathrm{d}\Omega - \int_{\Gamma_2} N_{\mathrm{f}}^{\mathrm{t}}\underline{\tau}\,\mathrm{d}\Gamma - \int_{\Omega}[\mathbf{B}^{\mathrm{t}}\mathbf{D}\,\mathrm{d}\underline{\varepsilon}^{\mathrm{p}}]\,\mathrm{d}\Omega = 0 \tag{37}$$

The coupled governing equations, namely, equations (23), (27), (33) and (9) or (12) can thus be discretized spatially to produce, in matrix form

$$\begin{bmatrix} \mathbf{K}_{\mathrm{ll}} & \mathbf{K}_{\mathrm{lT}} & \mathbf{K}_{\mathrm{la}} & \mathbf{0} \\ \mathbf{K}_{\mathrm{Tl}} & \mathbf{K}_{\mathrm{TT}} & \mathbf{K}_{\mathrm{Ta}} & \mathbf{0} \\ \mathbf{K}_{\mathrm{al}} & \mathbf{0} & \mathbf{K}_{\mathrm{aa}} & \mathbf{0} \\ \mathbf{0} & \mathbf{0} & \mathbf{0} & \mathbf{0} \end{bmatrix} \begin{Bmatrix} u_{\mathrm{l}} \\ T \\ u_{\mathrm{a}} \\ \underline{u} \end{Bmatrix} + \begin{bmatrix} \mathbf{C}_{\mathrm{ll}} & \mathbf{C}_{\mathrm{lT}} & \mathbf{C}_{\mathrm{la}} & \mathbf{C}_{\mathrm{Tu}} \\ \mathbf{C}_{\mathrm{Tl}} & \mathbf{C}_{\mathrm{TT}} & \mathbf{C}_{\mathrm{Ta}} & \mathbf{C}_{\mathrm{Tu}} \\ \mathbf{C}_{\mathrm{al}} & \mathbf{C}_{\mathrm{aT}} & \mathbf{C}_{\mathrm{aa}} & \mathbf{C}_{\mathrm{Tu}} \\ \mathbf{C}_{\mathrm{ul}} & \mathbf{C}_{\mathrm{uT}} & \mathbf{C}_{\mathrm{ua}} & \mathbf{C}_{\mathrm{uu}} \end{bmatrix} \begin{Bmatrix} \dot{u}_{\mathrm{l}} \\ \dot{T} \\ \dot{u}_{\mathrm{a}} \\ \dot{\underline{u}} \end{Bmatrix} = \begin{Bmatrix} f_{\mathrm{l}} \\ f_{\mathrm{T}} \\ f_{\mathrm{a}} \\ f_{\mathrm{u}} \end{Bmatrix} \tag{38}$$

where $\mathbf{K}_{ij}$ and $\mathbf{C}_{ij}$ represent the corresponding matrices of the governing equation, $(i, j = \mathrm{l}, \mathrm{T}, \mathrm{a}, \mathrm{u})$.

For simplicity, it is convenient to re-write equation (38) as

$$\mathbf{K}\{\varphi\} + \mathbf{C}\left\{\frac{\partial \varphi}{\partial t}\right\} = \{f\} \tag{39}$$

where φ refers to the global unknown, that is $\{u_1 \ T \ u_a \ \underline{u}\}^T$.

To solve equation (39), one of the useful methods for transient problems is direct temporal integration. A general form of two level difference method is employed to discretize the governing equation temporally.[17] Therefore equation (39) can be written as

$$\mathbf{K}^{n+1/2}[\chi\{\varphi^{n+1}\} + (1-\chi)\{\varphi^n\}] + \mathbf{C}^{n+1/2}[\varphi^{n+1} - \varphi^n]/\Delta t = (1-\chi)\{R^n\} + \chi\{R^{n+1}\} \tag{40}$$

where χ is the integration factor, which defines the required time interval ($\chi \in [0, 1]$).

To solve the highly non-linear problem considered here, the integration factor χ is recommended as 1.0, $\mathbf{K}$, $\mathbf{C}$ and R are evaluated at the mid-interval value of the primary variables. The scheme thus becomes the implicit mid-interval backward difference algorithm.

Re-writing equation (40) in alternate notation yields

$$\mathbf{A}\{\varphi^{n+1}\} = \{F\} \tag{41}$$

where

$$\mathbf{A} = \mathbf{K}^{n+1/2} + \mathbf{C}^{n+1/2}/\Delta t \tag{42}$$

and

$$\{F\} = \{R^{n+1}\} + \mathbf{C}^{n+1/2}\{\varphi^n\}/\Delta t \tag{43}$$

Therefore a solution of φ^{n+1} is achievable, providing the matrix $\mathbf{A}$ and the vector F can be obtained. This is actually achieved by the use of an iterative solution procedure.

At the beginning of each time interval, the first estimate of φ^{n+1} is assumed to be chosen as the value at last time interval, i.e. φ^n. Thus the value of φ^{n+1} for the first iteration can be obtained by

$$\{\varphi_1^{n+1}\} = \mathbf{A}_1^{-1}\{F_1\} \tag{44}$$

where $\mathbf{A}_1$ and F_1 are calculated at the value of φ^n.

After the first iteration, it is possible to correct the mid-interval value of φ^{n+1} and evaluate the matrix $\mathbf{A}$ and the vector F at time level $n + \frac{1}{2}$. The iteration will continue until the values of φ^{n+1} converge.

Convergence is monitored between every successive solution and is deemed to have been achieved when the following criterion is satisfied.

$$\left|\frac{\varphi_{i+1}^{n+1} - \varphi_i^{n+1}}{\varphi_i^{n+1}}\right| \leqslant \xi$$

where i is the iteration level and ξ is the relative tolerance.

The time step increment is controlled by two factors, maximum iterations and minimum iterations. Should the actual number of iterations for convergence exceed the maximum specified,

the time step size is reduced. Likewise, should the iteration number be less than the minimum, the time step size will be increased. This procedure enables a variable time step size to be employed, which will benefit the analysis of heat and moisture transfer taking place over a long period of time but with more rapid variations taking place during the initial stages of the problem.

5. VERIFICATION EXERCISES

A series of exercises were designed to verify both the complete code COMPASS and various sub-sets of the overall theory. Details of the work performed are presented below.

5.1. One-dimensional transient liquid flow with Dirichlet boundary

The first exercise was aimed at confirming the ability of the program to solve a transient liquid flow problem. An example of pore water flow in a linear system of semi-infinite length porous medium column was simulated.

The initial liquid pressure of the porous medium is u_0, at time $t = 0$. The pressure on the face of the porous medium at $x = 0$ is raised to u_1, and maintained at u_1 for all times greater than zero. The initial and boundary conditions can be expressed as follows:

$$u_l(x, 0) = u_0 \tag{45}$$

$$u_l(0, t) = u_1 \tag{46}$$

$$u_1(\infty, t) = u_0 \tag{47}$$

The solution of the liquid flow equation with initial condition (45) and boundary conditions (46) and (47) is

$$u_l = u_0 + (u_1 - u_0)\left(1 - \mathrm{erf}\left(\frac{x}{\sqrt{(4\alpha t)}}\right)\right) \tag{48}$$

where erf is error function, α is the coefficient of the equation.

To achieve the finite element solution of the problem, a 20 cm long column of 100 eight noded isoparametric elements is employed. The time step size used for time integration is 1 s. Since the finite element mesh has a finite length, it cannot satisfy boundary condition (47). However, the correct solution is still obtained before the transient response reaches the boundary.

The results of u_l/u_1 at time = 1000 s is given in Figure 1. Comparison of results indicates a very good match.

A similar exercise to confirm the ability of the program to solve a transient air flow problem was performed and the same conclusion reached.

5.2. Axisymmetric elastic loading-deformation test

The second exercise was designed to verify loading-settlement on an axisymmetric soil column. A commercial FE program, PAFEC, was used to run the same test example. The final results of both programs were the same as shown in their output files.

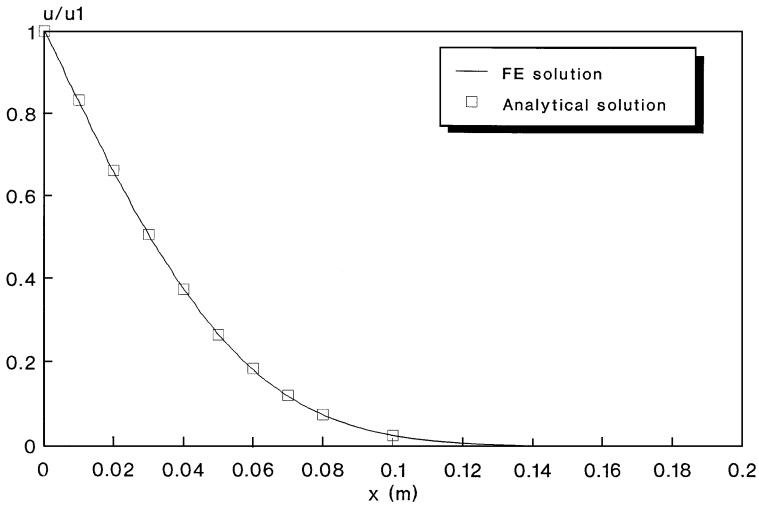

Figure 1. Comparison of FE and analytical solution—transient liquid flow

5.3. Axisymmetric heat transfer test

COMPASS was used to run a heat transfer test, the third exercise and compared with another in-house FE program (HEAT), which is a FE program for non-linear heat flow analysis of plane or axisymmetric problems. Both programs gave the same results for the test example.

5.4. Axisymmetric moisture transfer test with Neumann boundary

The fourth exercise was designed to check the ability of the program to solve moisture flow in an axisymmetric soil sample with Neumann boundary condition. Another in-house FE program was employed to run the same test example and both programs gave the same results.

5.5. Axisymmetric wetting-loading test—non-linear elastic state surface model

The fifth exercise was designed to verify the non-linear elastic state surface model when simulating wetting-loading in an axisymmetric soil column. The soil column is soaked from suction at 200 kPa to 100 Pa, and then the vertical stress is increased from 10 to 110 kPa keeping the suction constant. The results of volumetric strain and void ratio are plotted against vertical stress and suction respectively in Figures 2 and 3. During the wetting procedure, the soil sample shows swelling behaviour as illustrated in Figure 3. In the latter loading stage, the soil sample is compressed under the vertical load in Figure 2. The finite element results have been compared with those obtained directly from the analytical formulation. A very good match can be seen to have achieved.

5.6. Axisymmetric drying loading test—elasto-plastic model

COMPASS has been used to simulate a drying-loading case in unsaturated soil. The elasto-plastic model is employed. Two stress paths involved drying steps are considered here. The first

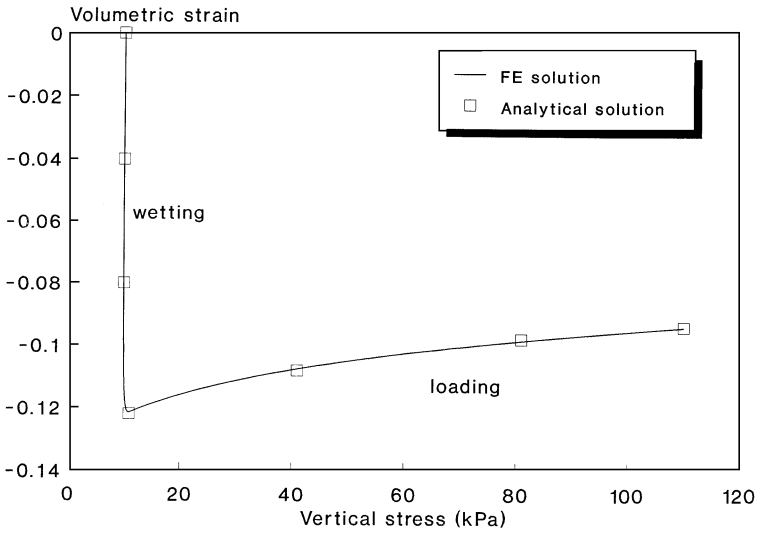

Figure 2. Comparison of FE and analytical solution—volumetric strain versus vertical stress

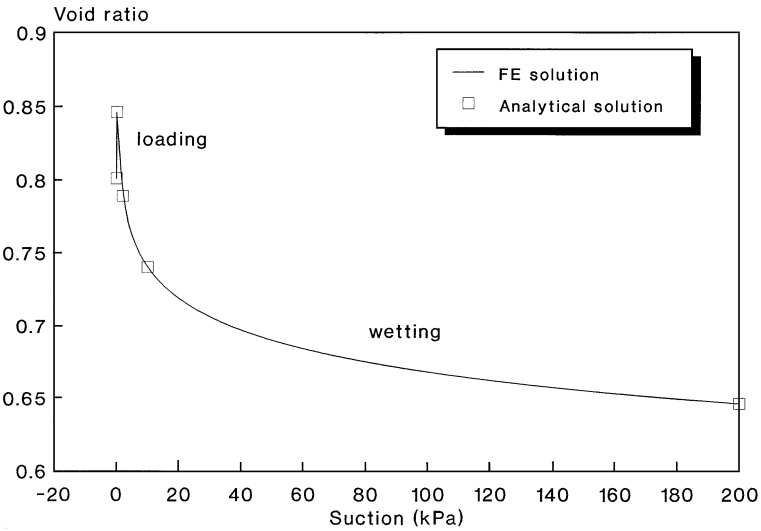

Figure 3. Comparison of FE and analytical solution—void ratio versus suction

one is loaded to 600 kPa under saturated conditions and then dried to a suction of 200 kPa. The second one is dried to suction of 200 kPa first, then loaded to 600 kPa. Due to the stiffness induced by suction increase, the second sample produces less volumetric deformation. The results of specific volume versus net mean stress is given in Figure 4. A very good match is obtained when the result from COMPASS is compared with that from the analytical formulation.

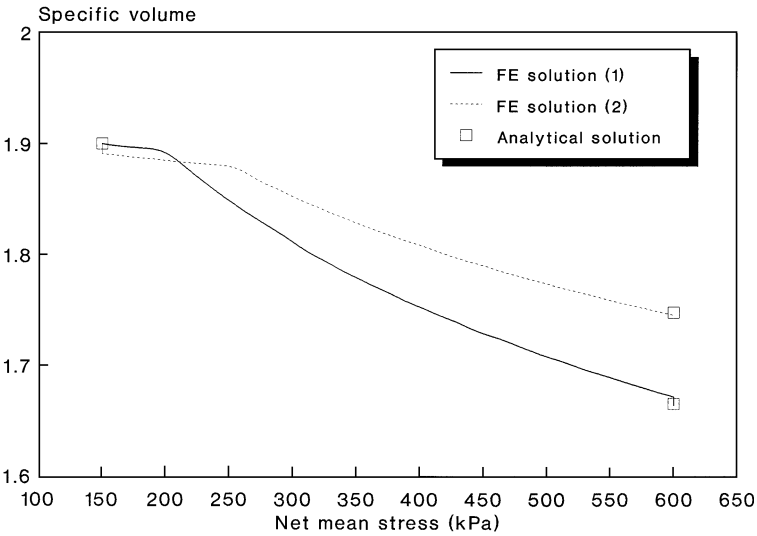

Figure 4. Comparison of FE and analytical solution—specific volume versus net mean stress

Apart from the above exercises, a number of numerical tests have been performed using plane stress and plane strain models. The results have been compared with either theoretical solutions or those obtained from a commercial FE package. All tests verified that the model is able to provide correct solutions. The model has also been used to analyse the consolidation of unsaturated soil, which includes the movement of moisture and deformation.[18] The results obtained were compared with another in-house FE program. Again a very good match was achieved.

6. APPLICATIONS

6.1. Isothermal moisture transfer at a constant air pressure

This section presents the application of the model to simulate an isothermal hydration experiment carried out by SCK/CEN, which involves the use of computerized X-ray tomography to measure hydration profiles in compacted plugs of powdered Boom clay.

The material employed in the research, namely Boom clay, is being considered as a suitable backfill and buffer material for the long-term safe disposal of high-level nuclear waste. Extensive experimental work has been carried out to determine the soil's thermo/hydraulic physical properties.

The Boom clay samples were produced by uniaxial compaction of the clay powder in the permeameter cell. After compaction the cell was left for 24 h to allow the sample to reach equilibrium conditions. To hydrate the sample the lower face of the clay plug was connected to a 1 m vertical column of water and the upper face was in contact with the atmosphere, allowing air to escape freely. During the hydration process X-ray tomographs were taken at 3 mm intervals along the clay plug and the mean water content each cross-section determined.

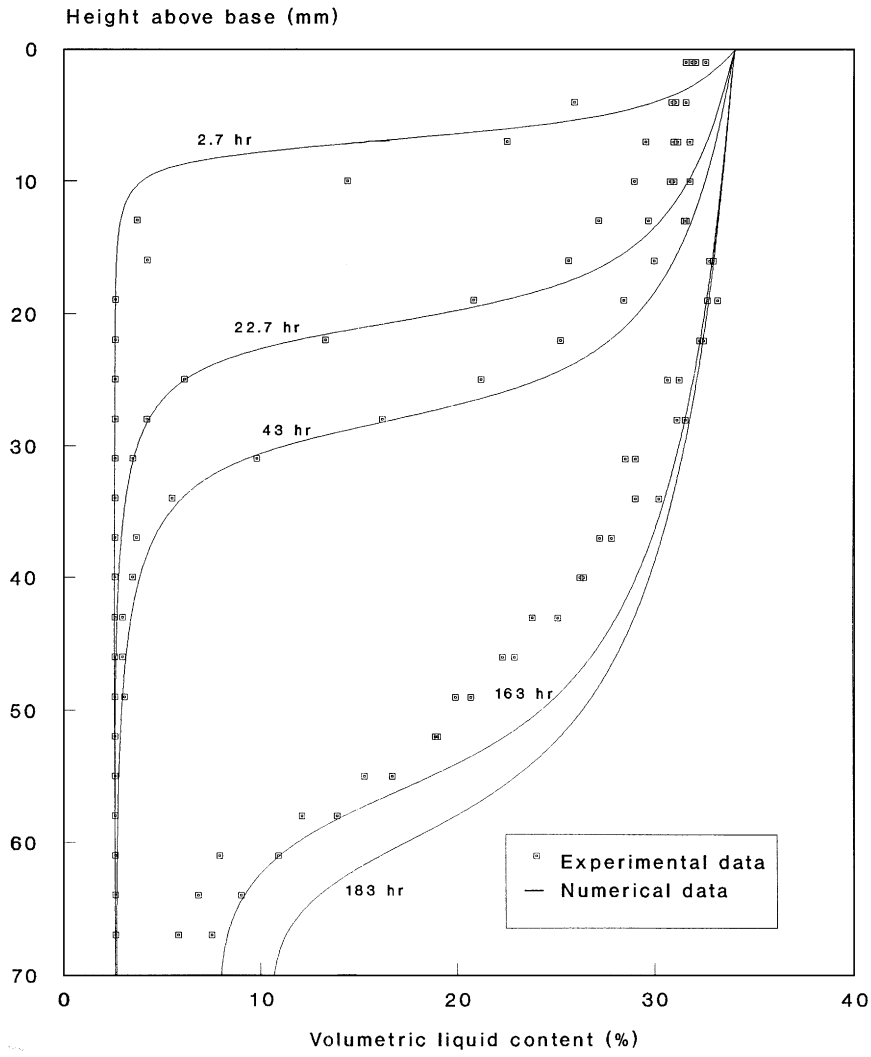

Figure 5. Comparison of numerical and experimental results—SCK/CEN hydration test at a constant air pressure

To apply the numerical model to the hydration experiment, thermo/hydaulic physical relationships, which were determined experimentally by SCK/CEN, are incorporated into the code.[18]

The domain was discretised into a one-dimensional mesh comprising 35×2 mm isoparametric elements and a constant time step size of 900 s was employed. The experimental and numerical results of the hydration experiment are given in Figure 5. The results of wetting profiles and penetration rate predicted by the numerical analysis are in good agreement with the experimental observations.

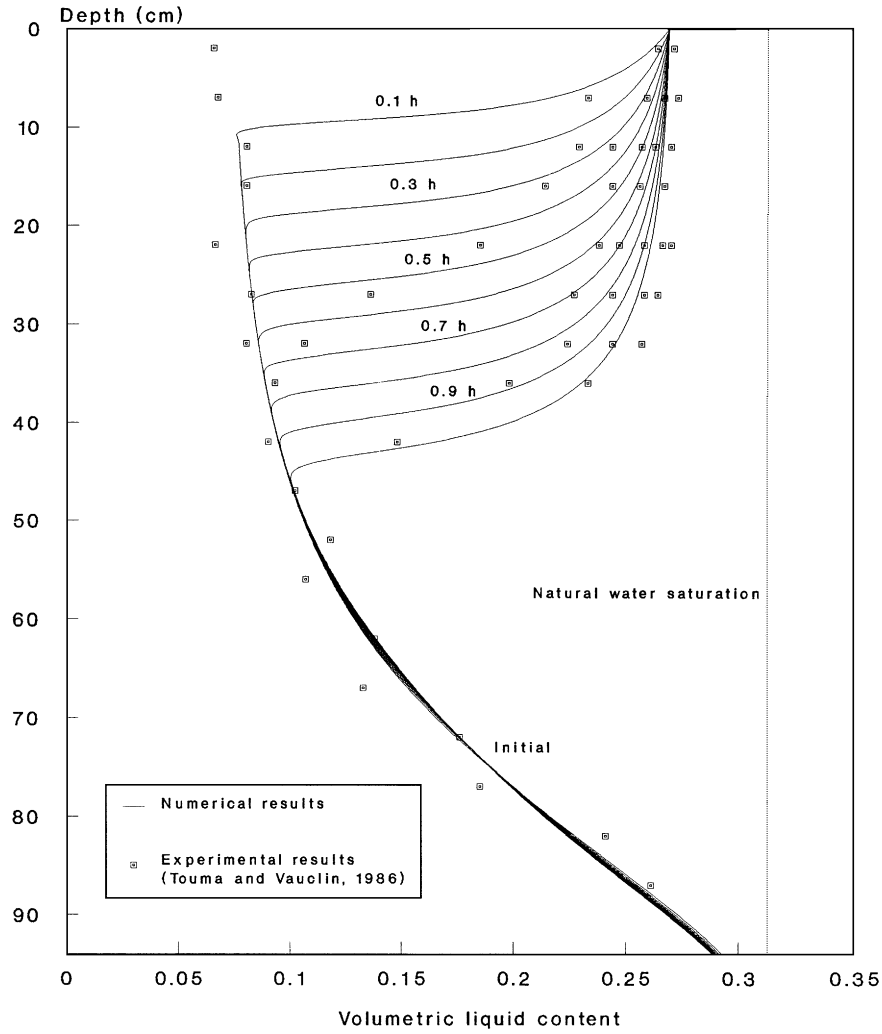

Figure 6. Comparison of numerical and experimental results—a two-phase infiltration test at varying air pressure

6.2. Coupled heat and moisture transfer at constant air pressure

Coupled heat and moisture transfer at constant air pressure has been investigated by comparison of numerical results with experimental results from a series of laboratory controlled heating experiments on medium sand. Excellent correlations were achieved.[5]

6.3. Isothermal moisture and air transfer

The isothermal air and moisture transfer subset of the model has been explored by comparison of numerical and experimental results of ponded infiltration into coarse sand[20] in Figure 6. Good agreement between the experimental and numerical results was achieved.[21]

The model has also been employed to simulate the coupled transport of energy, water and dry air in unsaturated alluvium by comparison with an alternative approach.[4] Good agreement between the two sets of results was observed for both the temperature and moisture distributions.

6.4. *Coupled heat, moisture and air transfer in a deformable soil*

The experimental work for this exercise was performed on an unsaturated Spanish montmorillonite clay by CIEMAT. The montmorillonite clay sample was uniaxially compacted at an initial water content of 12·4 per cent to a dry density of 1·62 g/cm^3 inside a stainless steel cell which is 14·6 cm high and 15 cm in inner diameter.[22] In the upper part of the cell, a heating device of 1·5 cm in height and 1·0 cm in diameter is placed along the axis of the cylinder and heated up to 100°C. The temperature distribution within the sample was measured by 9 thermocouples at different levels.

For the experiment reported here, steady state of temperature was reached around one hour after the heating started. At the end of the experiment, the clay sample was taken out and systematically cut to examine the final water content and dry density through the block.

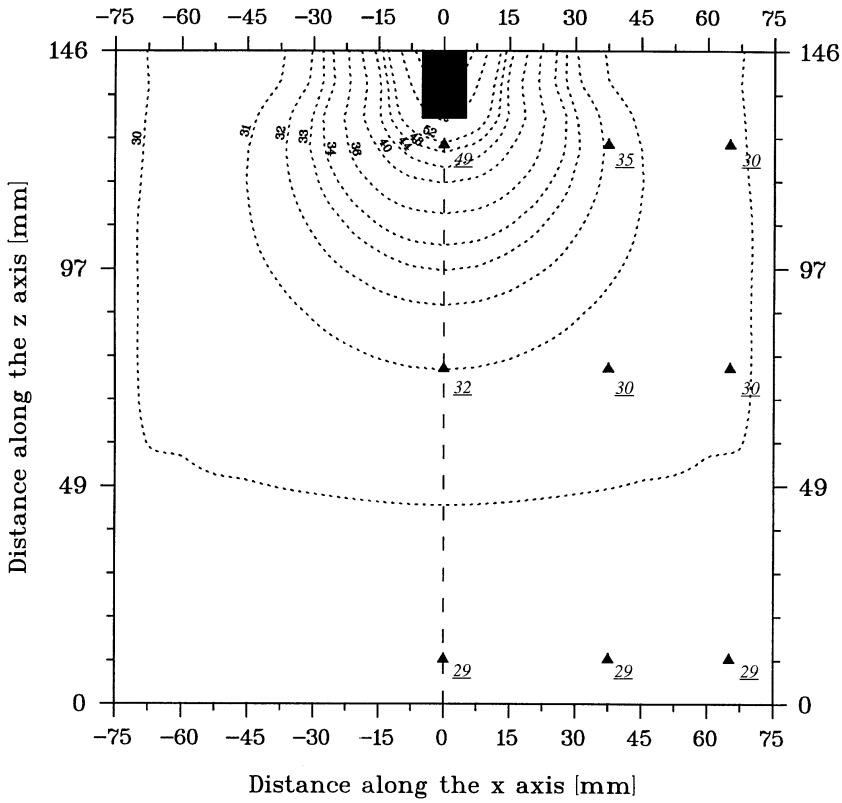

Figure 7. Comparison of numerical and experimental results—CIEMAT thermal test, plot of temperature

An axisymmetric finite element mesh, 146 mm high and 75 mm wide, was chosen to represent the test sample. The temperature is fixed at 100°C at the nodes of the heater. The temperature along the outside boundaries is fixed at 28°C due to the thermo-shower. Initial conditions for the simulation were estimated from measured experimental data.[23]

Examining the experimental and numerical results given in Figure 7, it can be seen that generally reasonable correlation is obtained. The overall pattern of temperature distributions are the same, with values at eight out of the nine experimental points quite well matched. The temperature response throughout all regions of the sample, both those near the heater and those near the boundary, is affected by a combination of the heat source itself and the applied boundary conditions. However regions near the boundary are more directly influenced by the temperature of the thermo-shower than the temperature of the heat source.

The results presented in Figures 8 and 9 are also claimed to be encouraging. A reduction in the degree of saturation and an increase in the void ratio near the heater occurred in the experiment. This pattern has been matched in the numerical simulation.[24,25] It is clear, however, that work is now required to further develop the numerical simulation so as to obtain improved correlation between numerical and experimental results.

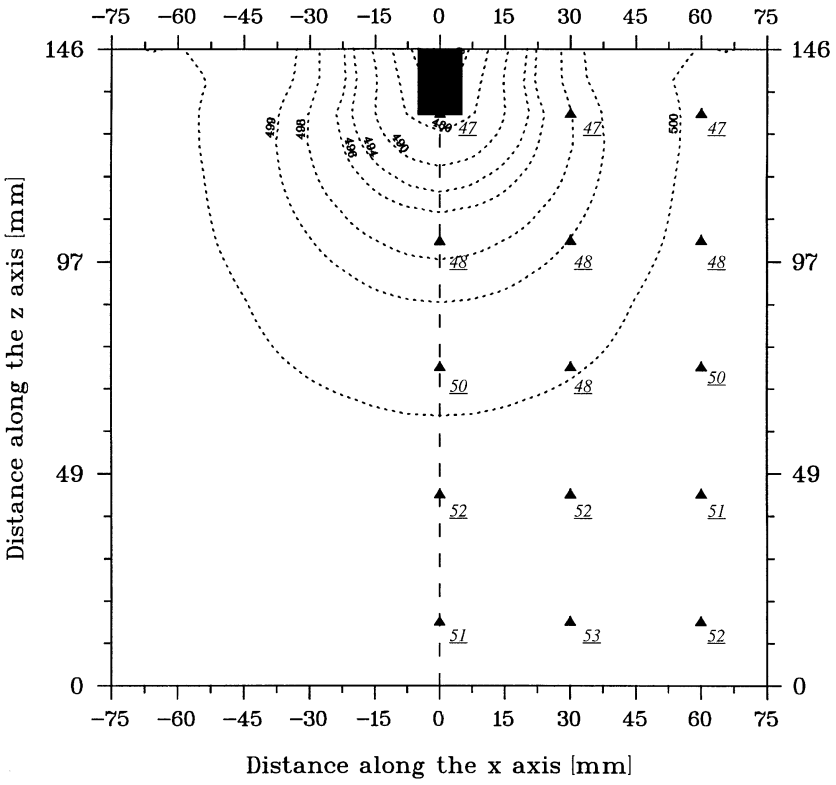

Figure 8. Comparison of numerical and experimental results—CIEMAT thermal test, plot of degree of saturation

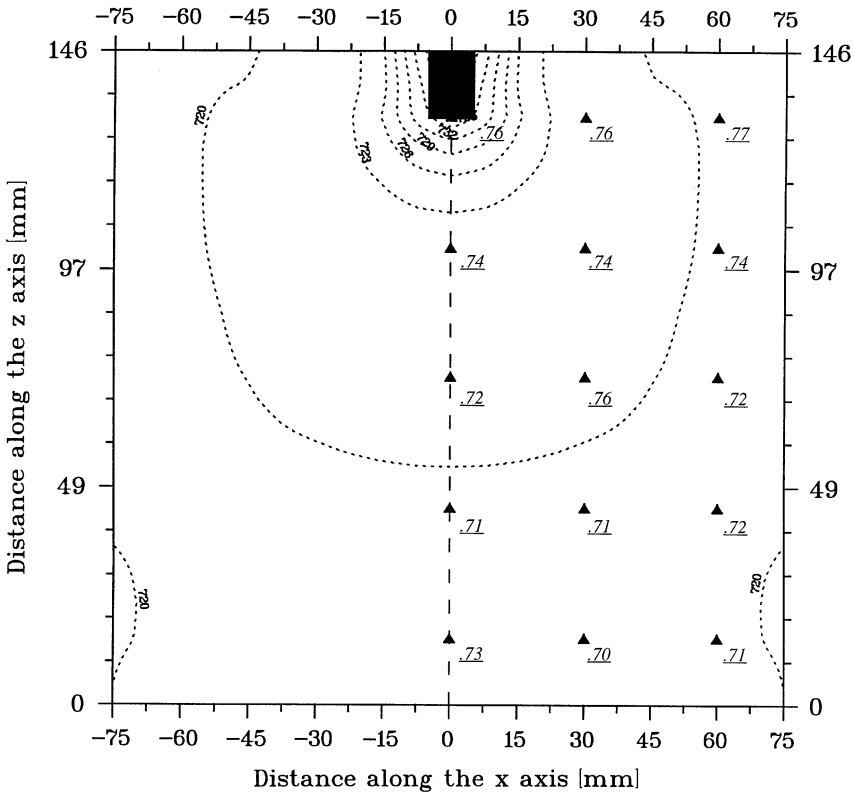

Figure 9. Comparison of numerical and experimental results—CIEMAT thermal test, plot of void ratio

6.5. Preliminary test results of the simulation of an in situ *test at AECL's Underground Research Laboratory (URL)*

In this exercise the model simulated a physical model, the *in situ* test of the isothermal experiment installed at URL. This experiment is being carried out at the 240 m level, i.e. 240 m below the surface, in crystalline rocks of the Canadian Shield. A 5 m deep, 1·24 m diameter borehole forms the basis for the experiment and is used to examine the water uptake by the buffer under *in situ* boundary conditions. The buffer's hydraulic and mechanical interactions with the surrounding rock and a concrete restraining plug is being monitored. This experiment is in progress. Typical results, comparing observed and simulated values of the pore water pressure head, using preliminary data, are presented in Figures 10 and 11 for 100 and 200 days, respectively, from the start of the experiment.

A reasonable agreement between predicted and measured data has been achieved at each time considered. The gradual resaturation of the buffer observed was also indicated by the simulated values. Differences exist, however, between observed and simulated values, particularly regarding the duration of the suction in the rock. The numerical analysis indicates that significant negative pressure heads can be generated in the granite. The magnitude of such pressure heads and the extent of their penetration into the granite then influences the rate of saturation of the

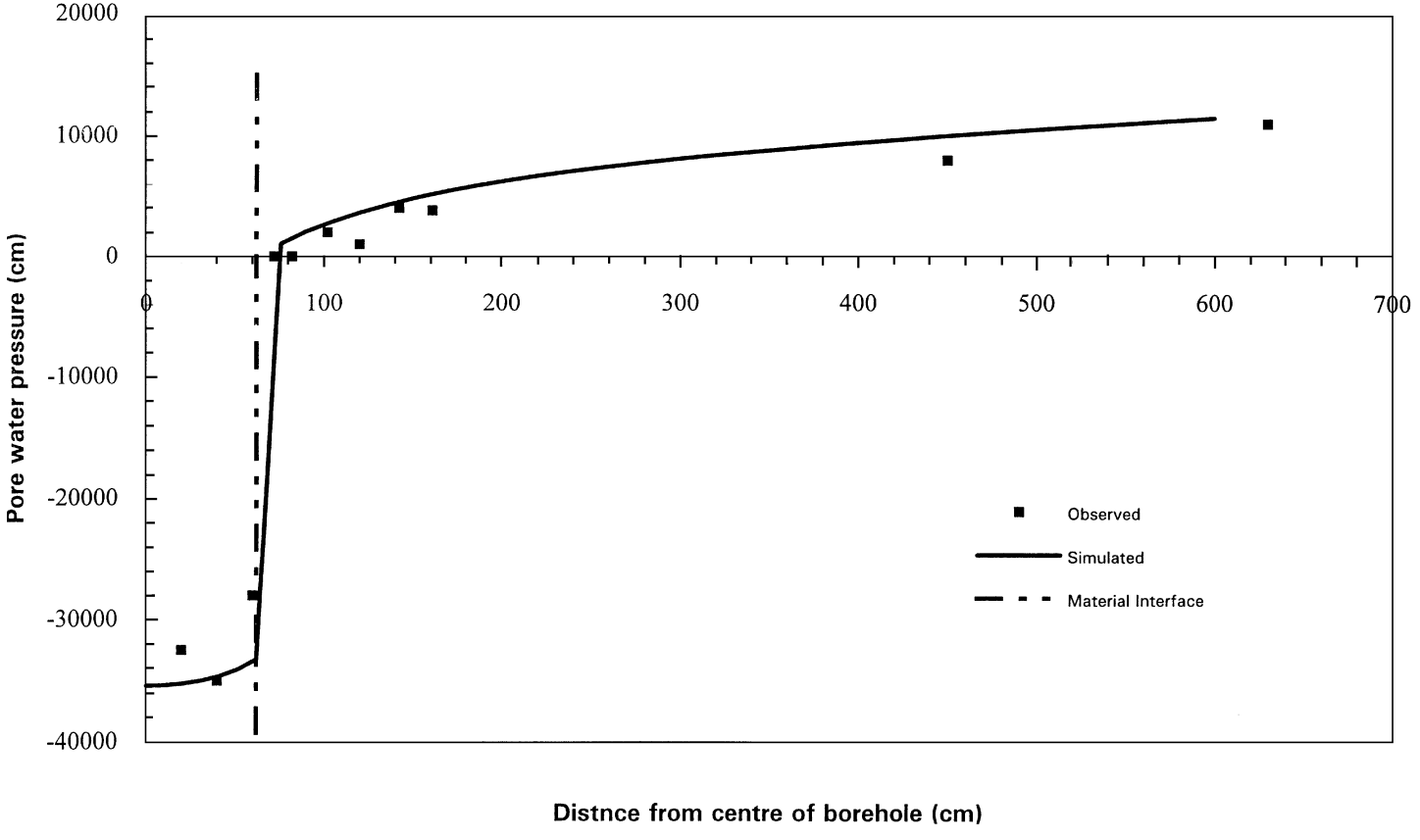

Figure 10. Comparison of numerical and experimental results—AECL isothermal experiment at URL after 100 days from the start of the experiment

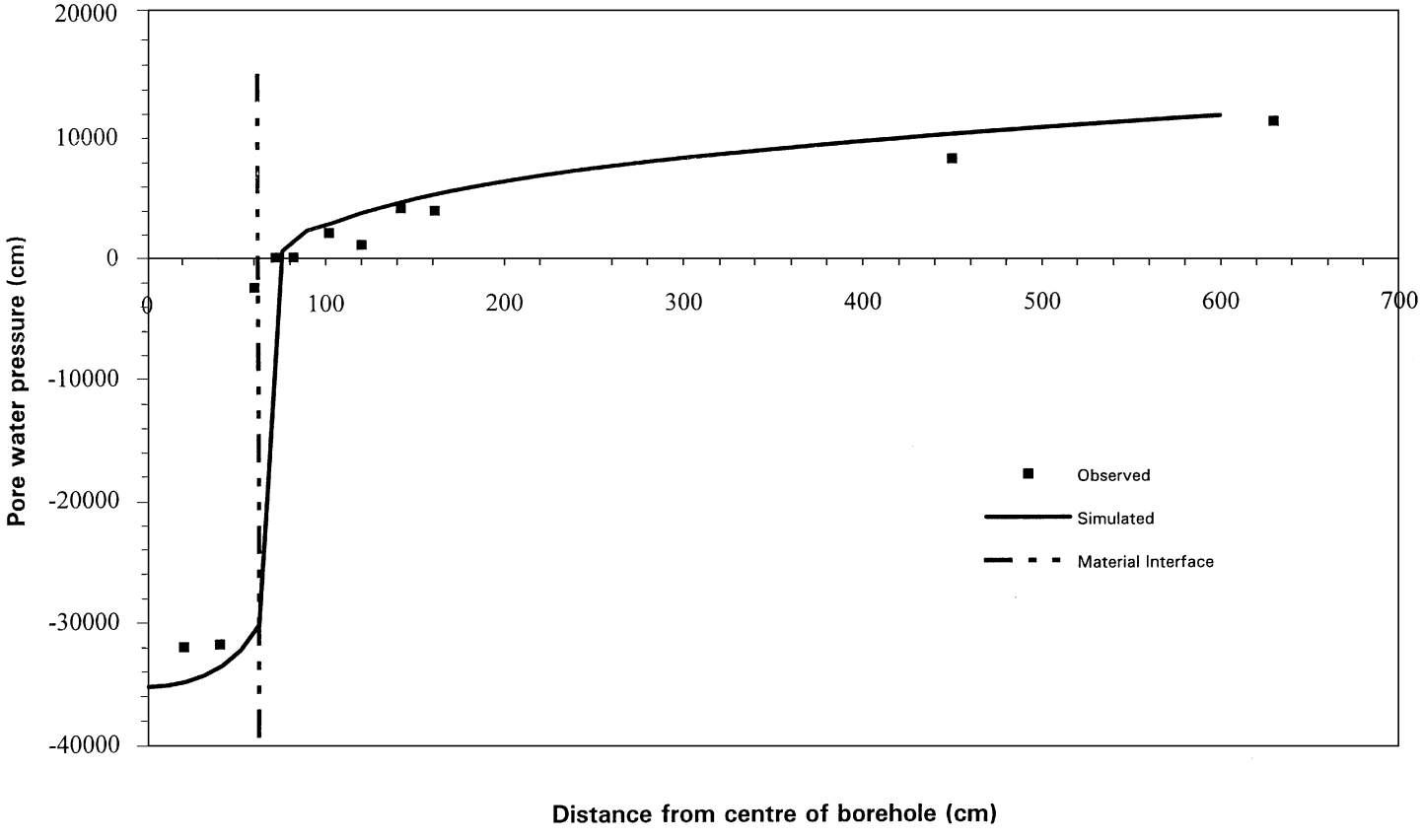

Figure 11. Comparison of numerical and experimental results—AECL isothermal experiment at URL after 200 days from the start of the experiment

bentonite-sand barrier. The simulation results obtained are strongly dependent on the hydraulic properties of the granite. High suction in the granite results in very low hydraulic conductivity in the near-field zone creating a nearly impermeable region. The modelling results serve to highlight the importance of buffer/rock hydraulic interaction and indicate the need for further investigation of the flow characteristics of the rock in the disturbed region near excavation.

Although it is still early in the validation programme, it is AECL's judgement that COMPASS seems to be a very useful tool that can successfully estimate the behaviour of clay engineered barriers. Their view is that the model is theoretically sound, includes the major coupled processes that take place in the near-field, and the results of preliminary tests suggest that the simulated values compare favourably with observed values from physical models.

7. CONCLUSIONS

The work presented in this paper describes first a model for the analysis of the coupled transport of heat, moisture and air transfer, which is applicable to a deformable unsaturated soil. The theoretical formulation and numerical implementation have been presented, which can accommodate either a thermoelastic constitutive relationship based on the state surface approach or an elasto-plastic model appropriate to describe unsaturated soil. A computer programme COMPASS for the solution of coupled thermo/hydro/mechanical boundary problem of unsaturated clay has been developed at Cardiff.

A number of tests have been carried out at the verification stage to ensure the accuracy of the computer code. Confidence in the numerical accuracy of the software has thus been obtained. A number of applications of the model have been performed to assess its ability to describe the physical phenomena involved. Further confidence in the model has therefore been achieved.

It is however recognized that further work is now required to investigate further the ability of the model to describe accurately the complex fully coupled phenomena under consideration. Good quality experimental data is limited and further work is necessary to provide such information, within a structured programme of validation tests.

The model described above has been developed from a mechanistic approach, combining together the various phenomena in an interrelated coupled manner. As such, the importance of validation of the new model is highlighted as a feature of importance. The development of the theoretical model and its numerical solution is seen as being fundamentally linked to a comprehensive on-going validation programme, in order to ensure the accuracy and practical usefulness of the work.

ACKNOWLEDGEMENTS

The work presented here carried out at Cardiff has been part funded from a research programme supported by the Commission of the European Union under Contract F12W-CT90-0033. This support is gratefully acknowledged, together with the collaboration of CIEMAT and SCK/CEN who performed some of the experiments. The Canadian Nuclear Fuel Waste Management Program is jointly funded by AECL and Ontario Hydro under the auspices of the CANDU Owners Group.

REFERENCES

1. J. R. Philip and D. A. de Vries, 'Moisture movement in porous materials under temperature gradients', *Trans. Am. Geophys. Union*, **38,** 222–232 (1957).
2. D. A. de Vries, 'Simultaneous transfer of heat and moisture in porous media', *Trans. Am. Geophys. Union*, **39**(5)**,** 909–916 (1958).
3. M. Geraminegad and S. K. Saxena, 'A coupled thermoleastic model for saturated-unsaturated porous media', *Geotechnique*, **36,** 539–550 (1986).
4. D. W. Pollock, 'Simulation of fluid flow and energy transport processes associated with high-level radioactive waste disposal in unsaturated alluvium', *Water Resour. Res.*, **22,** 765–775 (1986).
5. J. Ewen and H. R. Thomas, 'Heating unsaturated medium sand', *Geotechnique*, **39,** 455–470 (1989).
6. H. R. Thomas and S. D. King, 'Coupled temperature/capillary potential variations in unsaturated soil', *J. Engng. Mech., ASCE*, **117** (11)**,** 2475–2491 (1991).
7. H. R. Thomas and C. L. W. Li, 'Modelling transient heat and moisture transfer in unsaturated soil using a parallel computing approach', *Int. J. Numer. Anal. Methods Geomechanics*, **19,** 345–366 (1995).
8. E. E. Alonso, A. Gens and D. W. Hight, 'Special problem soils-general report' (seession 5), *Proc. 9th European Conf. Soil Mech. and Found. Engng.*, Dublin, 1987, pp. 1087–1146.
9. E. E. Alonso, A. Gens and A. Josa, 'A constitutive model for partially saturated soils', *Geotechnique*, **40,** 405–430 (1990).
10. D. G. Fredlung and H. Rahardjo, *Soil Mechanics of Unsaturated Soil*, Wiley, New York, 1993.
11. A. W. Bishop and G. E. Blight, 'Some aspects of effective stresses in saturated and partly saturated soils', *Geotechnique*, **13**(3)**,** 177–197 (1963).
12. D. G. Fredlung, 'Appropriate concepts and technology for unsaturated soils', *Canad. Geotech. J.*, **16,** 121–139 (1979).
13. A. Lloret and E. E. Alonso, 'State surfaces for partially saturated soils', *11th I.C.S.M.F.E.* Vol. 2, San Francisco, 1985, pp. 557–562.
14. E. L. Matyas, and H. S. Radhakrishna, 'Volume change characteristics of partially saturated soils,' *Geotechnique*, **18,** 432–448 (1968).
15. J. Bear and A. Verruijit, *Modeling Groundwater Flow and Pollution*, Reidel, Dordrecht, 1987.
16. E. E. Alonso, F. Batlle, A. Gens and A. Lloret, 'Consolidation analysis of partially saturated soils-application to earthdam construction', *Proc. 6th Int. Conf. on Num. Methods in Geomech.*, Innsbruck, 1988, pp. 1303–1308.
17. R. D. Cook, *Concepts and Applications of Finite Element Analysis*, Wiley, New York, 1981.
18. H. R. Thomas, Z. M. Zhou and Y. He, 'Analysis of consolidation of unsaturated soils', *Proc. Second Czechoslovak Conf. on Num. Meth. in Geomech.* vol. 1, Prague, 1992, pp. 242–247.
19. H. R. Thomas, M. R. Sansom, G. Volckaert, P. Jacobs and M. Kumnan, 'An experimental and numerical investigation of the hydration of compacted powered boom clay', in: I. Smith (ed.), *Numerical methods in Geotechnical Engineering*, A. A. Balkema, Rotterdam, 1994, pp. 135–142.
20. J. Touma and M. Vauclin, 'Experimental and numerical analysis of two-phase infiltration in a partly saturated soil', *Transport in porous media*, **1,** 27–55 (1986).
21. H. R. Thomas and M. R. Sansom, 'Fully coupled analysis of heat, moisture and air transfer in unsaturated soil', *J. Engng. Mech., ASCE*, **121**(3)**,** 392–405 (1995).
22. M. V. Villar, J. Cuevas, A. M. Fernández and P. L. Martin 'Effects of the interaction of heat and water flow in compacted bentonite', *Int. Workshop on Thermomechanics of Clays and Clay Barriers*, Bergamao, 1993.
23. M. V. Villar and P. L. Martin, 'Suction controlled oedometric tests in montmorillonite clay', *Proc. 29th Annual Conf. of the Engineering Group of the Geological Society of London*, 1993, pp. 337–342.
24. H. R. Thomas, Y. He, A. Ramesh, Z. Zhou, M. V. Villar and J. Cuevas, 'Heating unsaturated clay — an experimental and numerical investigation', in: I. Smith (ed.), *Numerical methods in Geotechnical Engineering*, 1994, A. A. Balkema, Rotterdam, pp. 181–186.
25. H. R. Thomas and Y. He, 'An analysis of coupled heat, moisture and air transfer in a deformable unsaturated soil', *Geotechnique*, **45,** 677–689 (1995).

